Nonlinear dynamics of magnetic and velocity field structures generated by multi-pulsing coaxial helicity injection in spherical torus plasmas

T. Kanki[1], M. Nagata[2], Y. Kagei[3]

[1]*Japan Coast Guard Academy, Kure, Japan*

[2]*University of Hyogo, Himeji, Japan*

[3]*Research Organization for Information Science & Technology, Tokai, Japan*

Refluxing approach of coaxial helicity injection (CHI) which operates in multi-pulsing CHI (M-CHI) has been proposed [1]. In the M-CHI scenario, current driven phase to perform the CHI by applying the gun voltage and decay phase to obtain the excellent confinement by partially decaying the plasma current and magnetic field are separated in time. Sustainment of the magnetic field of spheromak with a high electron temperature in quasi-steady state was for the first time demonstrated by the M-CHI in the SSPX device [2]. To explore the usefulness of the M-CHI for spherical torus (ST) configurations, the double pulsing operations have been tested in the HIST device, demonstrating the flux amplification and the sustainment of the ST [3]. The purpose of this study is to investigate the physical mechanism to rebuild the magnetic fields and to amplify the currents by using resistive nonlinear 3D-MHD simulations [4]. We focus our attention on the effects of the M-CHI on dynamics of the high-q ST.

The dynamics of the helicity–driven ST (HD-ST) usually involves the nonaxisymmetric helical distortion of a central open flux column (COFC) so that a 3D simulation geometry is essential to reproduce the distortion properly. All variables are treated in a normalized form. The length, magnetic field, and number density are normalized by the maximum length of the cylinder radius, L_0=0.5m, the strength of the characteristic magnetic field, B_0=0.2T, and the initial ion number density in the hydrogen plasma, n_0=5.0$\times 10^{19}$m^{-3}, respectively. Under these normalizations, the velocity and time are normalized by the Alfvén velocity, v_A=620km/s, and the Alfvén transit time, τ_A=0.81μsec, respectively. We adopt the simulation system shown in Fig. 1 and use a 3D full-toroidal cylindrical (r, θ, z) geometry. We divide the simulation region into two cylinders with a central conductor inserted along the symmetry axis. One is a gun region corresponding to a magnetized coaxial plasma gun region, and the other is a confinement region. The insertion of a toroidal field current I_{tf} along the geometry axis inside the central conductor produces a vacuum toroidal field, creating a tokamak configuration. In this paper, we set I_{tf}= 1.2 because we consider a high-q HD-ST configuration (q>2).

The governing equations to be solved in the simulation are the set of nonlinear resistive MHD equations. To solve the equations, we use the second-order finite differences method for the spatial derivatives and the fourth-order Runge-Kutta method for the time integration. The grid numbers are set to (N_r, N_θ, N_z)=(39, 64, 40) in the gun region and (N_r, N_θ, N_z)=(69, 64, 121) in the confinement region. A bias magnetic flux penetrates electrodes at the inner and outer boundaries of the gun region to drive the plasma current by applying an electric field.

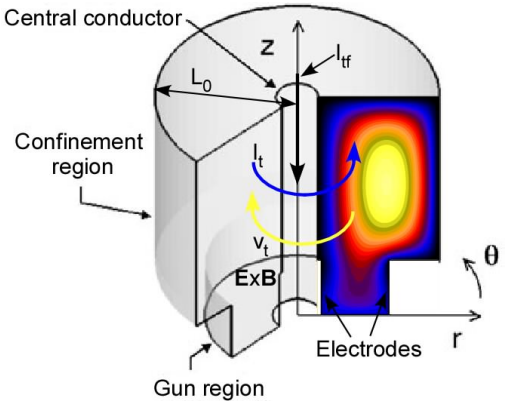

Fig. 1 Schematic view of simulation geometry in cylindrical coordinates (r, θ, z). Blue arrow indicates the direction of toroidal current I_t, and yellow arrow indicates that of toroidal velocity v_t and $\boldsymbol{E}\times\boldsymbol{B}$ plasma rotation.

We use a perfect conducting boundary at the wall of the confinement region. The initial conditions are given by an axisymmetric MHD equilibrium, which can be obtained by numerically solving a Grad-Shafranov equation under these boundary conditions. In the simulation, the mass density is spatially and temporally constant. The no-slip wall condition is assumed at all boundaries except for the gap between electrodes. The $\boldsymbol{E}\times\boldsymbol{B}$ drift velocity is given at the gap. We also impose that the heat flux can pass through all the boundaries.

On the basis of the simulation results, the mechanism to rebuild the magnetic fields is investigated. The poloidal flux contours of the axisymmetric MHD equilibrium with finite pressure gradients used as the initial condition are shown in Fig. 1. The conductivity $\kappa=1.0\times10^{-3}$, viscosity $\mu=1.0\times10^{-3}$, and resistivity $\eta=1.2\times10^{-4}$ are assumed to be uniformly constant throughout the entire region. A toroidally symmetric radial electric field E_{inj} of 1.0×10^{-2} is applied to the gap between gun electrodes in the shape of pulses. Figure 2 shows the time evolutions of the E_{inj}, toroidal current I_t, poloidal flux ψ_p, and magnetic energy W_{mag} for the toroidal Fourier mode. As shown in Fig. 2, I_t is successfully sustained against resistive dissipation during the driven phase. After E_{inj} vanishes at $t=200\tau_A$, I_t starts to decay due to the resistivity. When E_{inj} is applied again at $t=300\tau_A$, the I_t value increases from 0.35 up to 0.74 for about $100\tau_A$, resulting in the effective current amplification. However, the significant flux amplification is not observed from the time evolution of ψ_p because the current sheet which is generated by the plasmoid merging with the pre-existing HD-ST does not rapidly decay. In spite of applying E_{inj} at $t=300\tau_A$, the flux amplification does not occur at all, since the plasmoid cannot be ejected from the gun region due to the magnetic pressure of pre-existing HD-ST. The W_{mag} of the high-n modes is relatively large magnitude during the driven phase.

However, the fluctuation level of n=0 mode compared with other modes which has temporally constant value of about 4×10^3 is much larger. Thus the dynamics is almost axisymmetric. During decay phase, the n=1-5 components decrease, indicating to relax to an axisymmetric state. Figure 3 shows the time evolution of magnetic fields on the poloidal cross section. During the driven phase, the HD-ST causes a helical distortion of the COFC because of current flowing along the COFC. At t=912τ_A, the plasmoid starts to be ejected from the gun region due to the Lorentz force. At t=948τ_A, it is merged with the pre-existing HD-ST. As the result, the amplification of I_t and ψ_p occurs. After the plasmoid ejection, the closed field lines cannot be observed in the confinement region. During the decay phase, the closed field lines are regenerated there due to the dissipation of the magnetic fluctuation energy. At t=1167τ_A, the helical distortion of the COFC becomes small, and then ordered magnetic field structures are rebuilt. Figure 4 shows the time evolution of velocity fields on the poloidal cross section. During the driven phase, the strong poloidal flow v_z (=$E_r B_t$) moves from the gun to confinement region due to the Lorentz force. The vortices of the poloidal flow v_p are also caused around the upper confinement region by above v_z. From t=926τ_A to t=970τ_A, the negative toroidal flow v_t which is the same direction as I_t is driven around the COFC region by inductive toroidal electric field E_t(=-$v_z B_r$) because of the plasmoid ejection. After that, the positive v_t which is associated with the dynamo effect is generated around the COFC region. During the decay phase (t=1167τ_A), both v_t and v_p decay, and then the configuration approaches a static MHD equilibrium of HD-ST due to the dissipation of magnetic fluctuations to rebuild the closed field lines. Just after turning off the E_{inj} (t=1101τ_A), the v_p which moves from the confinement to gun region is caused by the pressure gradients The vortices of v_p then expands all over not only confinement region but also gun region.

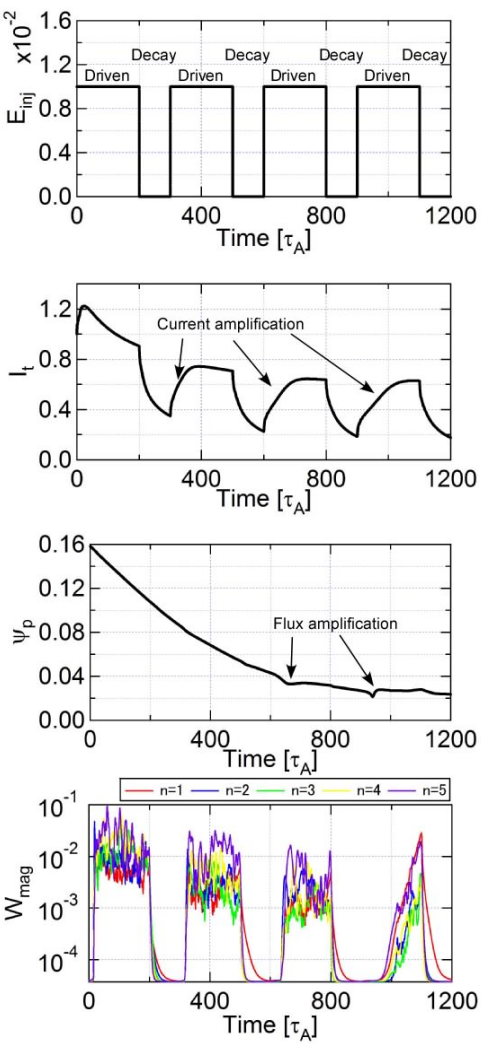

Fig. 2 Time evolutions of toroidal current I_t, poloidal flux ψ_p and magnetic energy W_{mag} when radial electric field E_{inj} is applied in the shape of pulses.

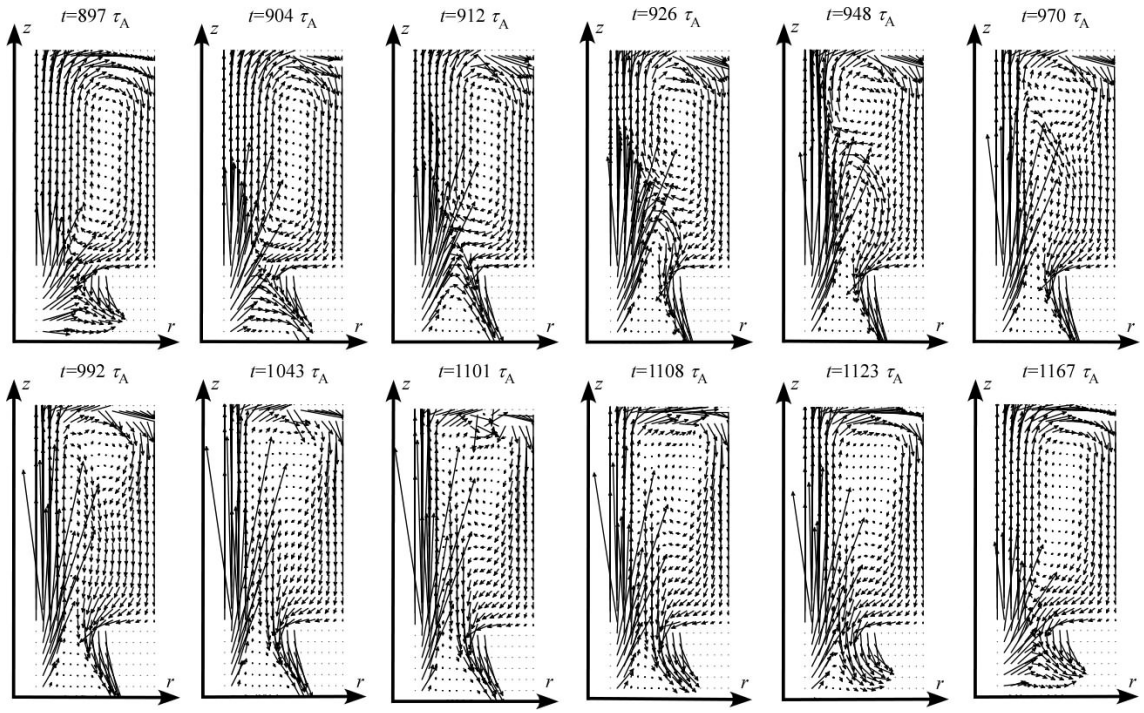

Fig. 2 Time evolution of vector plots of poloidal field B_p on the poloidal cross section at the θ=0 plane.

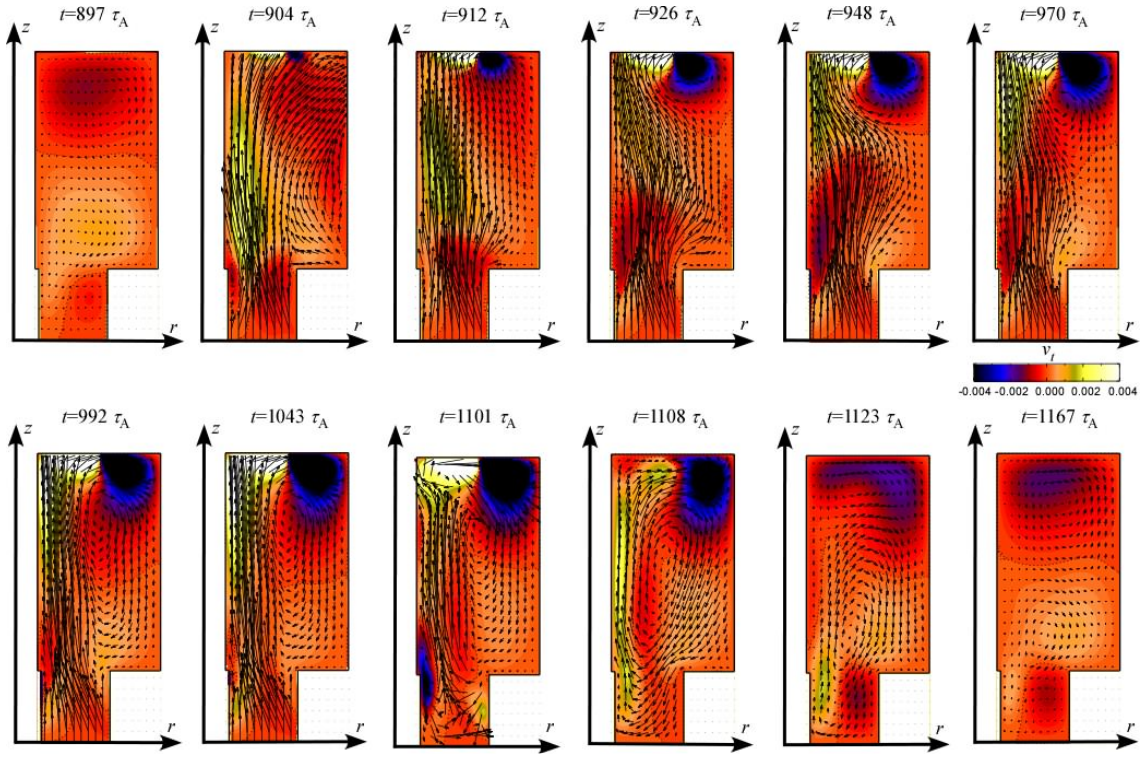

Fig. 3 Time evolution of vector plots of poloidal flow velocity v_p and contours of toroidal flow velocity v_t on the poloidal cross section at the θ=0 plane.

References

[1] E.B. Hooper, Plasma Phys. Control. Fusion **53**, 085008 (2011).

[2] B. Hudson *et al.*: Phys. Plasmas **15**, 056112 (2008).

[3] M. Nagata *et al.*, *Proc. 23rd IAEA Fusion Energy Conference* (Daejon, Korea, 10-16 Oct. 2010) EXC/P2-04.

[4] T. Kanki *et al.*, Plasma and Fusion Res. **5**, S2055 (2010).